

Electrophoretic mobility and colloidal stability of PLGA particles coated with IgG

M.J. Santander-Ortega, D. Bastos-González, J.L. Ortega-Vinuesa*

Biocolloid and Fluid Physics Group, Department of Applied Physics, University of Granada, Av. Fuentenueva S/N, 18071 Granada, Spain

Received 26 January 2007; received in revised form 23 May 2007; accepted 1 June 2007

Available online 14 June 2007

Abstract

Drug delivery systems based on polymeric nanocarriers have been widely exploited during the last years. However, one of the basic problems that is still not totally solved in this kind of systems is the ability of delivering drugs to specific target cells. Coating the nanocarrier with reactive antibodies against specific molecules presented in the external membrane of the target cells is a usual recommendation. In this paper, an ideal delivery system has been studied. Nanoparticles made of poly(D,L-lactic acid/glycolic acid) 50/50 (PLGA) polymers have been coated with polyclonal IgG. In the first part of the paper, some basic characteristics of these IgG–PLGA complexes have been analysed (i.e. size, electrophoretic mobility and colloidal stability). Then, the immunoreactivity of the immobilized IgG molecules was tested by using an optical device, monitoring the binding of a standard molecule (C-reactive protein, CRP) to the antibody (antiCRP–IgG) adsorbed on the PLGA particles. This allowed us to estimate the percentage of active IgG molecules on the PLGA particles by applying a simple kinetic model to the immunoreactivity results. According to this model, the PLGA–IgG particles supply a good immunoresponse even if only less than 5% of the total IgG molecules on the surface were active. Despite the simplicity of the system, the results may be of potential interest for developing more realistic nanocarriers with targeting ability. That is, it can be inferred that it is possible to obtain a high targeting specificity in IgG-sensitized nanocarriers even working with a low coverage of *active* antibody molecules. The results have been compared with those similarly obtained with polystyrene (PS) particles used as a reference system. © 2007 Elsevier B.V. All rights reserved.

Keywords: PLGA; Colloidal stability; Immunoassay; IgG; Nanocarriers

1. Introduction

A major effect in the pharmaceutical field has been caused by the use of colloidal dispersions of biodegradable polymers as nanoparticle drug carriers. This kind of systems, which emerged around 30 years ago, appears to be very promising to carry drugs, proteins or DNA molecules to specific organs within the body [1]. However, since the conception of this idea, a great deal of information about the potential and limitations of nanoparticles as drug carriers has been gathered. There is a general agreement about what the ideal carrier system must possess, which includes some specific common features, i.e. (i) the size of the particles must be in the nanometric scale (≤ 200 nm) in order to be capable of crossing diverse biological barriers; (ii) the external shell must be hydrophilic enough to evade the retic-

uloendothelial system (RES) and the mononuclear phagocytic system (MPS) and remain in the blood for a considerable amount of time and (iii) the particles must have reactive groups on the surface to be converted to stimuli responsive carriers that target to specific receptor ligands. In the case of carrying hydrophobic drugs, the use of hydrophobic particles becomes necessary to attain an appropriate drug load due the drug–polymer compatibility [2]. In these cases, the carrier particles must be made of a hydrophobic core that protects the drug from degradation and a hydrophilic shell (made of PEG, poloxamer or poloxamine derivatives) that prevents the recognition of the nanocarrier by the MPS cells. With regard to the targeting properties, the use of specific antibodies immobilized on the particle surface has become a feasible strategy usually recommended by numerous scientists.

The present work has been designed to model a simple drug delivery system with targeting ability. The particles have been made of poly(D,L-lactic acid/glycolic acid) 50/50 (PLGA) polymers, which is a material that has been extensively and

* Corresponding author. Tel.: +34 958 240018; fax: +34 958 243214.
E-mail address: jlortega@ugr.es (J.L. Ortega-Vinuesa).

successfully used in colloidal drug carriers [3–15]. In order to turn the hydrophobic PLGA surface into a hydrophilic one, the adsorption of a polypropylene oxide (PPO) and polyethylene oxide (PEO) tri-block copolymer (poloxamer) was performed in a previous work [16], where the colloidal stability of the PLGA–poloxamer complexes was also evaluated. In the present work, however, the potential capacity of PLGA nanoparticles to serve as specific reactive systems is studied. It should be noted that Kim et al. [17] have already developed PLGA particles with targeting specificity, although in this case specificity was obtained using a folate conjugate against folate receptors, which usually are overexpressed in cancer cells. Nevertheless, the use of immobilized antibodies in PLGA carriers is a targeting strategy that has not been sufficiently exploited at the present. In this paper, polyclonal IgG molecules have been adsorbed onto the PLGA particles in order to initially study some basic characteristics of these complexes, i.e. the electrophoretic mobility and colloidal stability. Subsequently, the targeting properties of the particles against any potential receptor have been analyzed by means of immunoprecipitation studies. C-reactive protein (CRP) has been used as a standard target molecule. Our goal in this point has been centred on quantifying the reaction between the adhered immunoreactive antibody with the target analyte in solution. It has been possible to estimate how many anti-CRP–IgG molecules remain active after their adsorption onto the PLGA surface by modelling the kinetics of CRP–antiCRP–IgG reactions using particle enhanced optical immunoassays. Although this is a simple system, the results obtained in this work may be of potential interest for the development of real drug carriers for *in vivo* studies. It should be noted that most of the results have been compared with those similarly obtained with polystyrene (PS) particles; PS–IgG complexes can be considered as a reference system, since they have extensively been used in numerous latex enhanced immunoassays during the last decades [18–21].

2. Materials and methods

2.1. PLGA nanoparticles

The poly(D,L-lactic acid/glycolic acid) 50:50 (PLGA) polymer was purchased from Boehringer-Ingelheim, under the commercial name of Resomer[®] RG 503. Its average molecular weight was 35,000 Da. The PLGA nanoparticles were prepared in our labs by a modified emulsion-solvent diffusion technique. First, 50 mg of PLGA was dissolved in 2 mL of dichloromethane and this organic solution was mixed for 30 s with 0.2 mL of pure water by vortex (2400 min⁻¹, Heidolph). This first volume of water is in pharmaceutical applications used to dissolve drugs to be incorporated in the particles. Then, the obtained emulsion was poured under moderate magnetic stirring onto a larger polar phase (25 mL ethanol), leading to immediate polymer precipitation in the form of nanoparticles. This sample was diluted with 25 mL MilliQ water and the stirring was maintained for 10 more minutes. Finally, the organic solvents (both ethanol and dichloromethane) were eliminated under vacuum at 30 °C (Rotavapor Büchi R-114, Flawil). The mean hydrody-

namic diameter of the PLGA particles was obtained by photon correlation spectroscopy using a 4700c System (Malvern Instruments, UK), and it was equal to 210 nm.

2.2. PS nanoparticles

The polystyrene (PS) latex particles were synthesized, cleaned and characterized by the Ikerlat S.A. Laboratories (Spain). In order to maintain the same superficial charged groups as those existing in the PLGA particles, a carboxylic PS latex was chosen. The size of this PS sample was 260 nm and its polydispersity index was equal to 1.008.

2.3. Other materials

Different proteins have been used in this work: human C-reactive protein (CRP), bovine serum albumin (BSA) and polyclonal pre-immune immuno- γ -globulin (IgG) were purchased from Sigma. Polyclonal antiCRP–IgG was obtained, purified and kindly donated by Biokit S.A. (Spain). The isoelectric point (iep) of both polyclonal IgG samples was determined by isoelectric focusing, and it was in the 6.0–7.9 range. All other solvents and chemicals used were of the highest grade commercially available.

2.4. IgG adsorption

The adsorption of IgG molecules onto PLGA and PS particles followed the same procedure, which is described below. A small volume of the stock latex suspensions (containing a PLGA or PS total area equal to 0.2 m²) was added to the protein solutions buffered at the desired pH. These buffered solutions presented a constant ionic strength of 0.002 M. Initially, the IgG concentration was in the 0–8 mg/m² range and the final volume of the samples was 8 mL. Incubation was carried out in a thermostatic bath where samples were gently agitated at 25 °C for 12 h. After incubation, samples were centrifuged and the supernatant filtered using a polytetrafluoroethylene filter (Millipore, pore diameter equal to 100 nm). The protein concentration in solution was determined, before and after adsorption, by direct UV spectrophotometry at $\lambda = 280$ nm ($\sum_{\text{IgG}} = 1.40 \text{ mL mg}^{-1} \text{ cm}^{-1}$), and then, the adsorbed amounts were calculated by subtracting the final from the initial values.

2.5. Electrophoretic mobility

The electrophoretic mobility measurements were carried out with a Zeta-Sizer IV (Malvern Instruments). The particles were diluted in the desired buffered solutions – all of them with ionic strength values equal to 0.002 M – for 10 min just before measuring. Final particle concentration was equal to $3 \times 10^9 \text{ mL}^{-1}$. The mobility data were taken from the average of six measurements at the stationary level in a cylindrical cell.

2.6. Colloidal stability

The aggregation of the latex particles immersed in different saline media was measured using a low-angle light scattering technique. In these experiments NaCl and CaCl₂ were used as aggregating salts. These experiments were carried out in an apparatus working with a He/Ne laser, using a rectangular scattering cell with a 2 mm path length, and measuring the light scattered at an angle equal to 10°. Equal volumes (1 mL) of salt and latex solutions were mixed and introduced into the cell by an automatic mixing device. The initial particle concentration was set at $5 \times 10^{10} \text{ mL}^{-1}$, and the intensity (I) of the scattered light during aggregation was analyzed for 120 s. The linearity in the aggregation kinetics was relatively good at the beginning, and the initial slopes (dI/dt) were easily obtained for every experiment. That allowed us to estimate the stability ratio W (also called Fuchs factor), which can be calculated from the following expression:

$$W = \frac{(dI/dt)_r}{(dI/dt)_s} \quad (1)$$

where the $(dI/dt)_r$ term corresponds to the initial slope of rapid coagulation kinetics, while $(dI/dt)_s$ is the same parameter for a slow coagulation regime. The critical coagulation concentration (ccc) can be easily determined by plotting the logarithm of W versus the logarithm of the salt concentration and locating that point where $\log W$ reduces to zero.

2.7. Immunoassays

The optimum experimental conditions for the immunoassays were established in ref. [22]. All the assays were carried out in a standard medium, namely, BSA saline buffer (pH 8.0 borate (13 mM), NaCl (150 mM), NaN₃ (1 mg/mL) as preservative and BSA in a 1 mg/mL concentration). This buffer approximately simulates the pH and ionic strength values usually found in physiological fluids. The role played by the BSA molecules is to cover possible PLGA or PS bare patches to avoid particle bridging produced by an unspecific adsorption of the antigen (CRP) molecules. In addition, the adsorption of these albumin molecules significantly helps to increase the colloidal stability of our IgG–latex complexes at pH 8, avoiding any potential aggregation caused by saline effects in the immunoreaction medium. Immunoagglutination was detected by turbidimetry working with a spectrophotometer (DU 7400, Beckman) at a $\lambda = 570 \text{ nm}$. Nine hundred and fifty microliters of an antiCRP–IgG–latex suspension in BSA saline buffer were quickly mixed with 50 μL of a CRP solution, ranging a final CRP concentration from 0.025 to 10 $\mu\text{g/mL}$. The initial particle concentration for PLGA and PS was 4.9×10^{10} and $2.3 \times 10^{10} \text{ mL}^{-1}$, respectively. It should be noted that samples were colloidally stable in the BSA saline buffer, and thus, only when the antibody–antigen recognition occurred, the aggregation of the particles began. The increase in turbidimetry was then monitored for different times. Subsequently, the immunoagglutination kinetics were analyzed by using a kinetic model that will be deeply described in the next section. The experimental results were fitted to the theoretical model using a commercial computer program (Origin 7.0,

Microcal, MA, USA), in which a nonlinear least squares fitting method is applied.

3. Results and discussion

Despite PLGA and PS particles share the same superficial charged group, its hydrophobic/hydrophilic character may not coincide. It is well known that one of the most important driving forces that control protein adsorption is the hydrophobic interaction [23]. Therefore, before analysing the IgG adsorption, the relative hydrophobicity of PLGA and PS surfaces was estimated by means of contact angle measurements. A water drop was deposited on a flat surface made of dry and compressed PLGA (or PS) particles. The contact angle was measured by using a goniometric technique based on the ADSA algorithm described in ref. [24]. As expected, polystyrene gave a higher contact angle (82°) than PLGA (74°), which means that the former possess a higher hydrophobic character than the latter. As will be shown afterward, this feature will be the main responsible of the differences observed in the protein adsorption experiments.

The maximum amount of adsorbed IgG as a function of the medium pH was then studied. Fig. 1 shows the obtained results when using independently PLGA and PS as adsorbent materials. Both curves are qualitatively similar, although significant differences appear quantitatively, since adsorption in PS approximately triples that found in the PLGA sample. As mentioned above, this could be caused by the different hydrophobic character shown by the two polymeric surfaces. It should be noted that IgG is a “soft” globular protein, for which hydrophobic interactions exert a great influence on adsorption [25,26]. It is suggested that hydrophobic interaction comes from the entropy increase when structured water molecules located in the vicinity of hydrophobic components are released to the bulk after the protein–surface contact [27]. Therefore, for a given soft protein, the higher the hydrophobicity of the substrate, the higher the protein adsorption. This explanation based on hydrophobic attraction also justifies the IgG adsorption observed at $\text{pH} \geq 8$, where electrostatic interactions between IgG molecules and par-

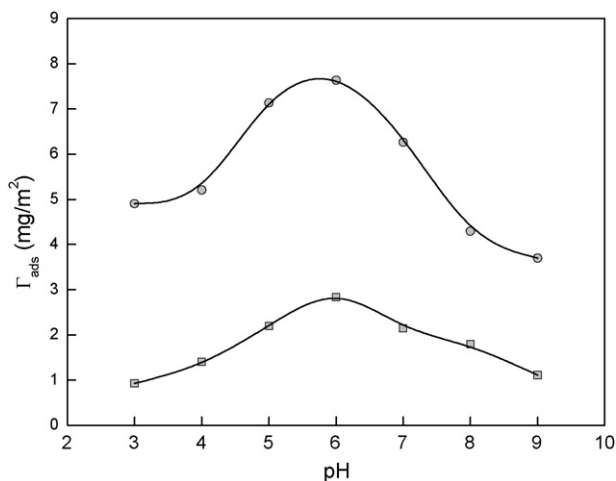


Fig. 1. Maximum amounts of polyclonal IgG adsorbed on PS (○) and PLGA (□) particles as a function of pH.

ticle surface are repulsive. Nevertheless, although hydrophobic interactions play an important role in the protein adsorption, it must be noted that electrostatic forces also participate, above all in low ionic strength media. For example, the maximum in the IgG adsorbed amount observed around pH 6, which almost coincides for both systems, is a result of electrostatic effects. The maximum position is usually obtained near the iep of the protein, although it is slightly shifted toward more acid pHs for negative adsorbent surfaces and toward more basic pHs for positive ones [28–30]. In fact, this maximum matches the isoelectric point of the protein–latex complex, which can be experimentally obtained by electrophoretic mobility measurements. At pH values far from the iep of the protein, the molecules are identically charged, and thus, they repel each other; in addition, they are more distended due to internal electrostatic repulsions, which subsequently give higher *area per molecule* values. Both contributions make the adsorption decrease. Besides, if the sign of charge of the adsorbent surface and the protein also coincide, the adsorption will be hindered even more. On the contrary, at pH 6 the sign of charge of particles and IgG differs, and thus, there is a favourable electrostatic attraction between the PLGA (or PS) surface and the IgG molecules. In addition, as this pH is near the iep of the protein, the inter- and intra-molecular repulsive interactions are still low; this is why the maximum adsorption is obtained at this pH value in both samples.

The electrophoretic mobility (μ_e) of the IgG–PLGA and IgG–PS complexes as a function of pH is shown in Fig. 2a and b, respectively. These measurements were carried out with particles having different protein load. A hypothetical mobility for the IgG molecules has also been depicted (dotted line). Such IgG μ_e data have been obtained from interpolating the mobility results of a cationic and an anionic PS latex totally covered with polyclonal IgG [28]. The mobility of the bare particles reflects the weak acid character of the carboxylic groups located on both PLGA and PS surfaces. Protonation at acid pHs produces charge cancellation which gives low mobility values. This feature is more patent in the PLGA particles than in the PS sample. When particles are covered with IgG, the mobility tends to approach to that expected for the pure protein, although such a value is not attained. The higher the protein load, the more the approximation. It is worthy to remark the low μ_e values obtained for the complexes with high IgG coverage. This suggests that, if only the overlap of electric double layers (but not steric hindrance effects) participates in the colloidal stability of the particles, the stability must be low in the pH 4–9 range.

In another set of experiments, the colloidal stability was evaluated at pH 4 (where the complexes presented a positive net charge), 6 (at which they were practically uncharged) and 8 (negatively charged particles) using NaCl and CaCl₂ as aggregating agents. Fig. 3 shows a representative experiment where the stability factor of IgG–PLGA and IgG–PS particles as a function of salt concentration is depicted at pH 8. The ccc values of different complexes at different pH values are shown in Tables 1a and 1b for the PLGA and PS samples, respectively. Let us first discuss the results found in acidic media. At pH 4, IgG–PLGA complexes had a low mobility (see Fig. 2a), which would mean a relatively low stability, provided that the

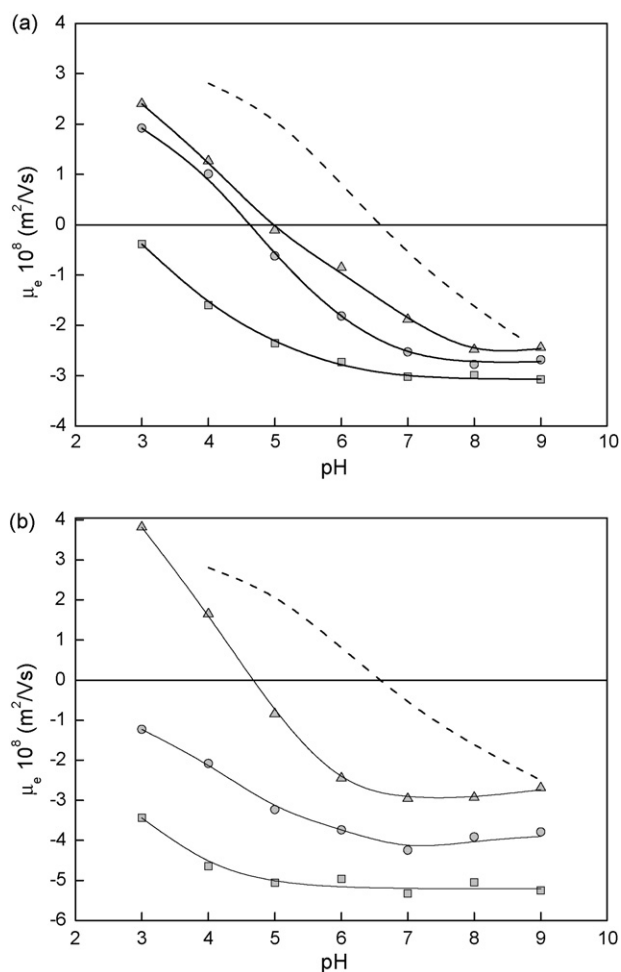


Fig. 2. Electrophoretic mobility vs. pH for (a) IgG–PLGA and (b) IgG–PS particles. Bare particles (\square); intermediate protein coverage (\circ): $\Gamma_{\text{PLGA}} = 1.9 \text{ mg/m}^2$ and $\Gamma_{\text{PS}} = 2.1 \text{ mg/m}^2$; high protein coverage (Δ): $\Gamma_{\text{PLGA}} = 2.9 \text{ mg/m}^2$ and $\Gamma_{\text{PS}} = 6.5 \text{ mg/m}^2$. Dashed line: hypothetical electrophoretic mobility of IgG molecules.

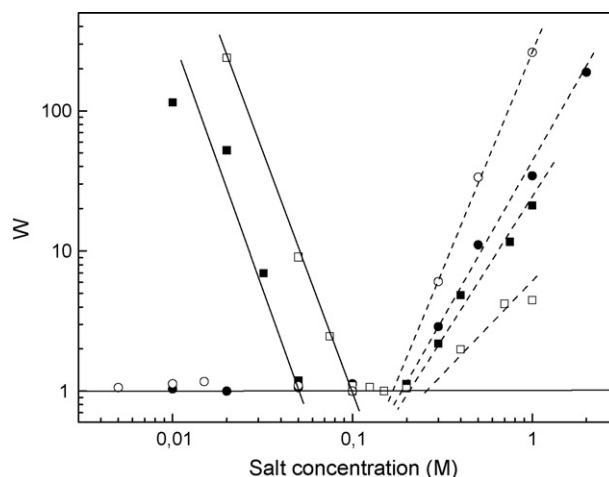


Fig. 3. Stability factor vs. salt concentration using NaCl (squares) and CaCl₂ (circles) as aggregating electrolytes. Open symbols and solid symbols represent IgG–PLGA (2.5 mg/m²) and IgG–PS (5.1 mg/m²) particles, respectively. Solid lines serve to guide the eye toward the corresponding ccc values. Dashed lines serve to locate the critical stabilization concentration (csc) in restabilization phenomena. Measurements were carried out at pH 8.

Table 1a

Critical coagulation concentrations (ccc) and critical stabilization concentrations (csc) of different IgG–PLGA complexes given in mM units

pH	IgG load (in mg/m ²)	NaCl ccc/csc	CaCl ₂ ccc/csc
4	0.7	70/–	45/–
4	1.7	90/–	65/–
6	1.9	<5/–	<5/235
6	2.9	Aggr.	Aggr.
8	0.9	150/–	<5/–
8	2.5	90/275	<5/170

Data were collected using different pH and protein load values, which are indicated in the first column.

stability depended exclusively on the electric characteristics (ζ -potential) of the particles. As expected, the ccc values at pH 4 correlates with the mobility data at this pH, that is, the stability was low (<100 mM), having the IgG–PLGA complex with more adsorbed protein (1.7 mg/m²) higher stability than that complex with lower protein load (0.7 mg/m²). In addition, the aggregating power of CaCl₂ is stronger than NaCl due to the double valence of calcium. The same reasoning can be applied to the IgG–PS complexes, where those particles with the highest protein load (5.2 mg/m²) had a significant stability, while those with an intermediate IgG coverage (3.1 mg/m²) were completely unstable even in absence of salt. This last pattern can be

Table 1b

Critical coagulation concentrations (ccc) and critical stabilization concentrations (csc) of different IgG–PS complexes given in mM units

pH	IgG load (in mg/m ²)	NaCl ccc/csc	CaCl ₂ ccc/csc
4	3.1	Aggr.	Aggr.
4	5.2	350/–	225/–
6	2.1	110/–	<5/–
6	6.5	55/–	<5/–
8	2.1	460/–	18/255
8	5.1	50/215	<5/195

Data were collected using different pH and protein load values, which are indicated in the first column.

explained if pH 4 would correspond to the iep of this complex, which is more than likely taking into account the data shown in Fig. 2b. It should be noted that the complexes used for the mobility and the stability experiments differ in the protein load (2.1 and 3.1 mg/m², respectively), and this is why no iep equal to pH 4 is directly observed in Fig. 2b. Nevertheless, considering the electrophoretic behaviour of the IgG–PS samples, it is plausible to expect an iep around pH 4 for the 3.1 mg/m² complex. The mobility data also serves to explain the stability patterns observed at pH 6. This pH corresponds with the iep of the IgG–PLGA particles, which is translated into an extremely low stability. However, the IgG–PS complexes are more stable, since its corresponding μ_e values differ from zero. It is worthy to highlight the important destabilizing effect caused by the divalent cation (calcium) when it acts as a counterion, giving ccc values lower than 5 mM. Finally, the ccc results obtained at pH 8 also can be justified according to the electrophoretic behaviour of the systems. Nevertheless, the most striking result observed at this basic pH 8 is the restabilization phenomenon found at high electrolyte concentrations. This stability cannot be explained by the ζ -potential values of the particles, since at high salt concentrations the electrical double layer is totally compressed. This restabilization mechanism has a structural origin based on the hydration forces that appear in hydrophilic surfaces [27]. A well-known interpretation of these hydration forces is that a polar (hydrophilic) surface induces an ordering of the solvent which exponentially decays away from the surface. The hydration of the surface reduces the free energy of the system. An overlap of the ordered-solvent layers near the two mutually approaching surfaces creates a structural force. Partial dehydration of the surface polar groups and the ions located near the interface due to the mutual approach will lead to an increase in the system energy, which results in a repulsive force [31]. The adsorption of the protein turns the original PLGA or PS hydrophobic surface into a hydrophilic one, where the hydrophilicity degree is governed by the protein coverage. This is why restabilization does not exist in bare latex particles (see Fig. 4a and b for PLGA and PS, respectively) or in those complexes with a

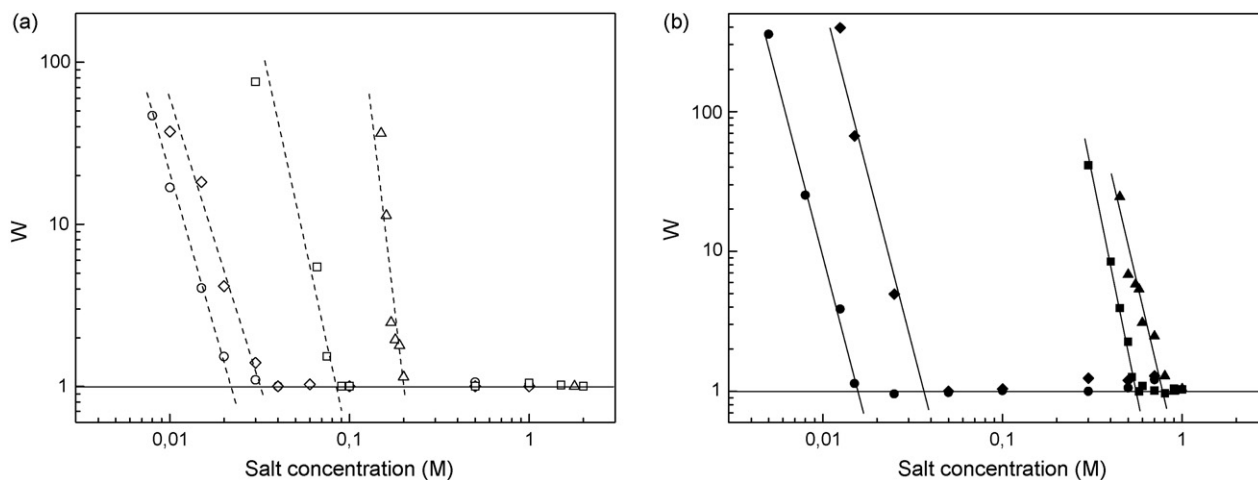


Fig. 4. (a) Stability factor of bare PLGA particles. NaCl at pH 4 (\square) ccc = 85 mM; NaCl at pH 8 (Δ) ccc = 200 mM; CaCl₂ at pH 4 (\circ) ccc = 20 mM and CaCl₂ at pH 8 (\diamond) ccc = 30 mM. (b) Stability factor of bare PS particles. NaCl at pH 4 (\blacksquare) ccc = 550 mM; NaCl at pH 8 (\blacktriangle) ccc = 800 mM; CaCl₂ at pH 4 (\bullet) ccc = 15 mM and CaCl₂ at pH 8 (\blacklozenge) ccc = 35 mM.

low IgG load. It should be noted that hydration forces does not only depend on the surface hydrophilicity, but also on the nature and concentration of the hydrated counterions that surround the particles. The critical stabilization concentration (csc) is defined as the minimum salt concentration at which restabilization starts. These csc data are also shown in Tables 1a and 1b. As cations are more hydrated than anions, hydration forces are usually observed in negatively charged systems, where the cations acts as counter ions. This is why restabilization is observed at pH 8 but not at pH 4. Finally, as calcium is a more hydrated cation than sodium, the restabilization power of the former is higher than that of the latter. Different authors have exhaustively studied this kind of hydration forces in colloidal systems; the interested reader can be found such information elsewhere [32–37].

In order to know if the adsorption process denatures the protein molecules – which would make the IgG–PLGA complexes completely useless for targeting purposes – the immunoreactivity of the adsorbed antibodies was performed. This kind of experiments allows us to test possible denaturation or unfavourable orientation of the molecules on the PLGA surface. Immunoreaction was then evaluated using CRP as a model target molecule and antiCRP–IgG–PLGA (and -PS) as reactive nanoparticles. In these experiments, the adsorption of antiCRP–IgG onto the particles was performed at pH 8. The IgG adsorbed amounts were 1.0 and 2.1 mg/m² for the PLGA and PS particles, respectively. It should be noted that immunoassays based on latex technology are usually performed at pH and ionic strength values reproducing the physiological conditions (pH ≈ 7.5 and *I* ≈ 150–170 mM). Under these conditions our IgG–PLGA (or -PS) particles were colloiddally unstable when they are totally coated with antibody (see in Table 1a the ccc value at pH 8 when PLGA particles have an IgG load equal to 2.5 mg/m², or see Table 1b for the 5.1 mg/m² complex in the PS case). A false positive would be obtained if the system aggregates in absence of the specific antigen. Therefore, it is necessary to work with stable particles that do not spontaneously coagulate at slightly basic pH and at 150 mM ionic strength media. There are different strategies to improve the stability of antibody–latex complexes, as reviewed in ref. [21]. One of the possible solutions is to co-adsorb a stabilizing molecule (a surfactant, a lipid or a protein) together with the antibody. The immunological reactivity depends on the latter, whereas the colloidal stability is a function of the former. This is why we have used in our experiment PLGA and PS particles partially coated by IgG (approximately 50% of the surface), instead of using nanospheres fully coated by antibody. In this way, there are PLGA and PS patches (free of IgG) available to adsorb the stabilizing molecule (BSA in our case). Therefore, the 1.0 and 2.1 mg/m² for the IgG loading on PLGA and PS particles, respectively, allowed us to obtain stable particles (due to the spontaneous BSA adsorption on the surface patches when particles are immersed in the reactive medium: *BSA saline buffer*), but maintaining a good immunoreactivity. Fig. 5 shows a typical immunoaggregation experiment. It should be noted that our particles were stable in the pure BSA saline buffer, and thus, they did not agglutinate in absence of CRP; therefore, they

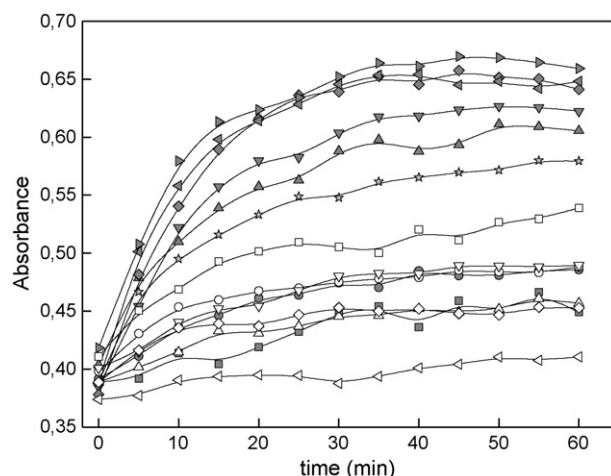


Fig. 5. Immunoagglutination kinetics of antiCRP–IgG–PLGA particles for different CRP concentrations (in mg/L): 0.025 (■); 0.05 (●); 0.1 (▲); 0.15 (▼); 0.2 (◆); 0.25 (◄); 0.5 (►); 1.0 (★); 2.0 (□); 3.0 (○); 4.0 (△); 5.0 (▽); 6.0 (◇) and 10.0 (◁).

only collapsed due to the bridging effect caused by the CRP after the corresponding antiCRP–IgG recognition. According to Fig. 5, the immunoagglutination was high at intermediate CRP concentrations, but low at high and low CRP concentrations. This feature becomes evident in Fig. 6a and b, where the absorbance increment versus CRP concentration is plotted for different time intervals. A typical bell-shape curve (also called *precipitine* curve) is obtained, which depends on the molar ratio of antigen to antibody [38,39]. For low CRP concentrations, few antigen molecules are available to bridge the IgG–latex particles, and thus, small agglutination kinetics are obtained. On the other hand, at high CRP concentrations, the active sites of the antibodies are rapidly saturated with different CRP molecules, and thus the bridging process, which only can take place when the same antigen molecule is recognized by IgG molecules adsorbed in two different particles, is hindered. A maximum in agglutination efficiency exists between these two extreme regimes. It is observed that IgG–PS complexes are more reactive at low CRP concentrations than those of PLGA. This feature has a simple explanation: the amount of IgG molecules adsorbed on the PS doubles that of PLGA, and thus, the immunosensitivity must be also higher, provided that the orientation of the IgG molecules was similar in both samples.

The immunoassay results can also allow us to estimate the percentage of active IgG on the latex particles. This can be performed by using a simple kinetic model for antigen–antibody reactions in particle-enhanced immunoassays developed by Quesada et al. [40–42]. The model proposed by these authors can be applied to immunoagglutination processes detected by nephelometry [40,41] or by spectrophotometry [42], although the basic equations slightly change depending on the optical technique. The model is based on the La Mer and co-workers idea [43,44], that says that the rate of agglutination must be equal to the product of the particle collision frequency and a collision efficiency factor which actually leads to aggregation of the particles (that is, to antibody–antigen binding). The model proposed by

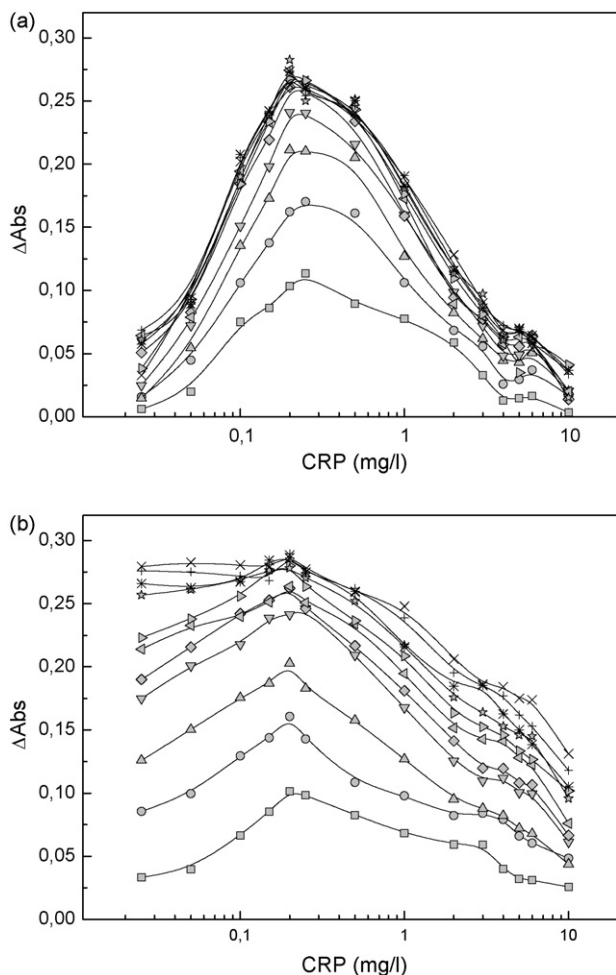


Fig. 6. Absorbance increment for the (a) IgG–PLGA and (b) IgG–PS systems vs. CRP concentration for different time intervals (in min): 5 (■); 10 (●); 15 (▲); 25 (▼); 30 (◆); 35 (◀); 40 (▶); 45 (☆); 50 (✱); 55 (+) and 60 (×).

Quesada et al. required some hypothesis to find a simple relationship between the kinetics constant of aggregation and the initial concentration of antigen into the reaction buffer. The model can be summarized as follows. Note that this is only a resume, and thus, details must be found elsewhere [40–42]. The model conceptually divides the immunoaggregation process into two steps. In the first one, the antibody–latex particles are in the solution and the antigen molecules are added; then, these last molecules become distributed between the solution and the antibody sites reaching an equilibrium state *before* latex flocculation. In the second step, the formation of bridges between spheres through antigen molecules begins. Although this simplistic mechanism could be questionable, it can be justified by the fact that protein (CRP) molecules are much smaller than latex nanospheres, so the former diffuse much faster than the latter. The master

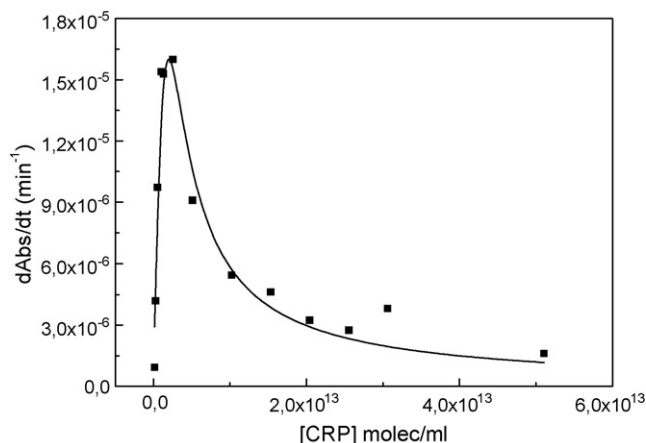


Fig. 7. Initial slope of the immunoagglutination kinetics vs. CRP concentration for the PLGA–IgG sample. Squares are experimental data, while the solid line represents the theoretical fitting that comes from applying the kinetics model. The “ C ”, “ K ” and “ n ” values used for this fitting are given in Table 2.

equation that relates the immunoagglutination kinetics (that is, the initial slope of the curves shown in Fig. 5— $d\text{Abs}/dt$) with the total number of immunologically active IgG molecules per particle (n) is shown below:

$$\frac{d\text{Abs}}{dt} = \frac{C}{4} \left(N_0 n + A + \frac{1}{K} - \sqrt{\Delta} \right) \left(N_0 n - A - \frac{1}{K} + \sqrt{\Delta} \right) \quad (2)$$

where

$$\Delta = \left(N_0 n + A + \frac{1}{K} \right)^2 - 4 N_0 n A \quad (3)$$

In Eq. (2), N_0 is the initial concentration of latex particles, A the initial concentration of antigen in the solution, K the equilibrium constant describing the interaction of the free antigen with the antibody adsorbed onto the latex surface and C is a parameter related to some optical characteristics and other factors (i.e. the particle diffusion coefficient, the electrostatic repulsion due to the overlap of the diffuse double layers of antigens and sensitized latex beads, the attractive interaction due to the London–van der Waals forces, etc.) [42]. Eq. (2) depends on three fitting parameters: n , K and C . Fig. 7 shows the experimental immunoagglutination results (symbols) of the PLGA sample fitted by Eq. (2) (solid line). As mentioned in Section 2, the experimental data were adjusted to Eq. (2) by using the Origin 7.0 programme, which used a nonlinear least squares fitting algorithm with three independent variables (n , K and C). The best fitting for the PLGA system was obtained with the n , K and C values shown in Table 2. The same analysis was performed for the PS sample, and the corresponding values are also shown

Table 2
Fitting parameters of the kinetics model and percentage of active IgG molecules on PLGA and PS particles

	$C/4$ (10^{-28} abs units $^{-1}$ mL 2 molecules $^{-2}$)	n (molecules/particle)	K^{-1} (10^{12} molecules mL $^{-1}$)	Active IgG (%)
PLGA	1.1 ± 0.6	21 ± 6	1.05 ± 0.20	3.8 ± 1.4
PS	1.9 ± 1.7	35 ± 5	1.05 ± 0.20	2.0 ± 0.3

in Table 2. The antigen–antibody equilibrium constant K must be equal in both cases, as obtained. In addition, the estimated K value is of the same order of magnitude as those found previously for other polyclonal IgG immunoreactions [40–42,45]. Nevertheless, the most interesting parameter to discuss is the number of active IgG molecules per particle (n). This parameter is higher for the PS sample than for the PLGA one, which agrees with the better immunoresponse shown by the former (see Fig. 6b, specially at low CRP concentrations) when compared to the latter (Fig. 6a). In addition, taking into account the particle surface area and the protein coverage, it is possible to calculate the percentage of active IgG molecules per particle. For example, a 210 nm diameter spherical PLGA particle possesses an area equal to $1.38 \times 10^{-13} \text{ m}^2$. Our IgG coverage (1.0 mg/m^2) can be translated into molecules per square meter – by knowing the antibody molecular weight (150,000 Da) and the Avogadro number – which was $4.015 \times 10^{15} \text{ molecules/m}^2$. Combining this last value with the calculated area per particle, one can determine the total number of IgG molecules per particle, which was 555 molecules/particle. According to the theoretical fitting, the number of active IgG molecules per particle – that is, the n parameter – was 21. This means that only around 4% of the total polyclonal IgG molecules are active and properly orientated outward for the PLGA sample. In the PS case, this results was even lower: 2%. Despite the n parameter indicates $n_{\text{PS}} > n_{\text{PLGA}}$, a lower value for the active IgG molecules in the PS particles is plausible. There are two factors that would contribute to reduce the percentage of reactive molecules in the PS particles. (i) On the one hand, the higher hydrophobicity of PS makes the surface–IgG hydrophobic interactions more intense, and thus, deformation of the adsorbed antibodies is favoured [23]; this partial denaturation reduces the native immunoreactivity. (ii) On the other hand, a high adsorption coverage – which is favoured in the hydrophobic PS surface – also contributes to diminish the percentage of active molecules. A crowded polyclonal IgG layer hinders the union of a voluminous antigen (as CRP, which has a MW = 114,000 Da) to any active IgG, simple by steric impediments caused by the presence of non-reactive IgG molecules placed at the vicinity of the active one. Nevertheless and despite these low values, the reactivity of both types of complexes was very good, as shown in Fig. 6a and b. This means that it is possible to develop drug delivery systems with appropriate targeting properties using few *active* IgG molecules per particle. This information could become very useful when monoclonal active IgG molecules instead of polyclonal ones were used; at least, the cost for sensitizing the nanocarriers with the antibody can be reduced, since few IgG molecules would be needed to produce stimuli responsive particles. In addition, the colloidal stability of the system can be easily improved in this situation, since there would be a lot of available surface to be coated by any stabilizer molecule, which would increase the poor colloidal stability observed with these particles when they are totally coated by polyclonal antibodies. It should be noted that coadsorbing other molecules (surfactants, lipids, proteins) that act as stabilizer agents together with the IgG is a general strategy used to improve the stability of antibody–latex particles [21]. At the present, we are using a biocompatible non-ionic surfactant

– a poloxamer (Pluronic[®] F68) – to enhance the stability of our IgG–latex complexes. These preliminary results obtained with a ternary system (PLGA–IgG–poloxamer) will be presented in a future paper.

4. Conclusions

PLGA nanoparticles have been sensitized with IgG molecules in order to experimentally simulate a simple drug delivery system with targeting ability. The corresponding electrophoretic mobility and colloidal stability have been subsequently studied. It has been proved that adsorption of polyclonal IgG produces a reduction of the stability of the particles around physiological pHs. Nevertheless, this handicap could be overcome if coadsorption of IgG and any stabilizer molecule was performed. In addition, the potential targeting ability has been quantified by measuring the immunoreactivity of the IgG–PLGA complexes. The analysis of the results by using a simple theoretical model has allowed us to estimate the percentage of active IgG molecules per particle. A low value around 4% has been found, which is acceptable taking into account that we have worked with a polyclonal sample. The obtained results can be useful to design future nanocarriers vectorized with IgG molecules in order to deliver drugs to specific target cells. At least, according to the results shown in this paper, a potential delivery system based on PLGA can be prompted: The use of monoclonal IgG molecules is advised, as all of them will be immunologically active against the same target molecule. In this case, low antibody coverage may be enough to achieve a PLGA carrier with high targeting ability. Subsequently, the bare PLGA patches must be coated by a non-ionic surfactant (i.e. Pluronic[®] F68). In this way, it would be possible to obtain immunoreactive stable particles that would also avoid recognition by the MPS cells.

Acknowledgements

Financial support from the “Comisión Interministerial de Ciencia y Tecnología” Project MAT2003-01257 (European FEDER support included) and from the “Consejería de Innovación, Ciencia y Tecnología de la Junta de Andalucía” Project FQM 392 is gratefully acknowledged.

References

- [1] S.J. Douglas, S.S. Davis, L. Illum, *CRC Crit. Rev.* 3 (1987) 233.
- [2] M.J. Alonso, in: S. Cohen, H. Bernstein (Eds.), *Microparticulate Systems for the Delivery of Proteins and Vaccines*, Marcel Dekker Inc., New York, 1996 (Chapter 7).
- [3] D.H. Lewis, in: M. Chasin, R. Langer (Eds.), *Biodegradable Polymers as Drug Delivery Systems*, Marcel Dekker Inc., New York, 1990 (Chapter 1).
- [4] A. Schade, T. Niwa, H. Takeuchi, T. Hino, Y. Kawashima, *Int. J. Pharm.* 117 (1995) 209.
- [5] M.D. Blanco, M.J. Alonso, *Eur. J. Pharm. Biopharm.* 43 (1997) 287.
- [6] T. Govender, S. Stolnik, M.C. Garnett, L. Illum, S.S. Davis, *J. Controlled Release* 57 (1999) 171.
- [7] R. Graf, M. Luck, P. Quellec, M. Marchand, E. Dellacherie, S. Harnisch, T. Blunk, R.H. Muller, *Colloids Surf. B* 18 (2000) 301.
- [8] Y.P. Li, Y.Y. Pei, X.Y. Zhang, Z.H. Gu, Z.H. Zhou, W.F. Yuan, J.J. Zhou, J.H. Zhu, X.J. Gao, *J. Controlled Release* 71 (2001) 203.

- [9] K. Avgoustakis, A. Beletsi, Z. Panagi, P. Klepetsanis, A.G. Karydas, D.S. Ithakissios, *J. Controlled Release* 79 (2002) 123.
- [10] J. Panyam, V. Labhasetwar, *Adv. Drug Deliv. Rev.* 55 (2003) 329.
- [11] N. Csaba, L. González, A. Sánchez, M.J. Alonso, *J. Biomater. Sci. Polym. Ed.* 15 (2004) 1137.
- [12] S.S. Feng, L. Mu, K.Y. Win, G.F. Huang, *Curr. Med. Chem.* 11 (2004) 413.
- [13] M.L.T. Zweers, G.H.M. Engbers, D.W. Grijpma, J. Feijen, *J. Controlled Release* 100 (2004) 347.
- [14] C.E. Astete, C.M. Sabliov, *J. Biomater. Sci. Polym. Ed.* 17 (2006) 247.
- [15] E. Ricci-Junior, J.M. Marchetti, *J. Microencapsulation* 23 (2006) 523.
- [16] M.J. Santander-Ortega, A.B. Jódar-Reyes, N. Csaba, D. Bastos-González, J.L. Ortega-Vinuesa, *J. Colloid Interface Sci.* 302 (2006) 522.
- [17] S.H. Kim, J.H. Jeong, K.W. Chun, T.G. Park, *Langmuir* 21 (2005) 8852.
- [18] A. Kondo, T. Kawano, F. Itoh, S. Higashitani, *J. Immunol. Methods* 135 (1990) 111.
- [19] C.P. Price, D.J. Newman, *Principles and Practice of Immunoassay*, Stockton Press, New York, 1991.
- [20] J.L. Ortega-Vinuesa, J.A. Molina-Bolívar, J.M. Peula, R. Hidalgo-Álvarez, *J. Immunol. Methods* 205 (1997) 151.
- [21] J.L. Ortega-Vinuesa, D. Bastos-González, *J. Biomater. Sci. Polym. Ed.* 12 (2001) 379.
- [22] J.L. Ortega-Vinuesa, J.A. Molina-Bolívar, R. Hidalgo-Álvarez, *J. Immunol. Methods* 190 (1996) 29.
- [23] W. Norde, *Adv. Colloid Interface Sci.* 25 (1986) 267.
- [24] O.I. del Río, A.W. Newmann, *J. Colloid Interface Sci.* 196 (1997) 136.
- [25] R.D. Milton, C.R. Robertson, *Langmuir* 7 (1991) 2710.
- [26] P. Warkentin, B. Wälivaara, I. Lundström, P. Tengvall, *Biomaterials* 15 (1994) 786.
- [27] J.N. Israelachvili, *Intermolecular and Surface Forces*, Academic Press, London, 1992.
- [28] F. Galisteo-González, J. Puig, A. Martín-Rodríguez, J. Serra-Domènech, R. Hidalgo-Álvarez, *Colloids Surf. B* 2 (1994) 435.
- [29] J. Buijs, J.W.T. Lichtenbelt, W. Norde, J. Lyklema, *Colloids Surf. B* 47 (1995) 633.
- [30] J.L. Ortega-Vinuesa, M.J. Gálvez-Ruiz, R. Hidalgo-Álvarez, *Langmuir* 12 (1996) 3211.
- [31] S. Leikin, A.A. Kornyshev, *Phys. Rev. A* 44 (1991) 2.
- [32] J.N. Israelachvili, G.E. Adams, *J. Chem. Soc., Faraday Trans.* 74 (1978) 975.
- [33] R.M. Pashley, *Adv. Colloid Interface Sci.* 16 (1982) 57.
- [34] J.A. Molina-Bolívar, F. Galisteo-González, R. Hidalgo-Álvarez, *Colloids Surf. B* 21 (2001) 125.
- [35] N.V. Churaev, B.V. Derjaguin, *J. Colloid Interface Sci.* 103 (1985) 542.
- [36] J.A. Molina-Bolívar, F. Galisteo-González, R. Hidalgo-Álvarez, *Phys. Rev. E* 55 (1997) 4522.
- [37] J.A. Molina-Bolívar, J.L. Ortega-Vinuesa, *Langmuir* 15 (1999) 2644.
- [38] M. Heidelberger, F.W. Kendall, *J. Exp. Med.* 62 (1935) 467.
- [39] R.P.O. Tengerdy, *J. Immunol. Methods* 99 (1967) 126.
- [40] M. Quesada, J. Puig, J.M. Delgado, J.M. Peula, J.A. Molina, R. Hidalgo-Álvarez, *Colloids Surf. B* 8 (1997) 303.
- [41] J.A. Molina-Bolívar, F. Galisteo-González, M. Quesada-Pérez, R. Hidalgo-Álvarez, *Colloid Polym. Sci.* 276 (1998) 1117.
- [42] M. Quesada, J. Puig, J.M. Delgado, R. Hidalgo-Álvarez, *J. Biomater. Sci. Polym. Ed.* 9 (1998) 961.
- [43] R.H. Smellie, V.K. La Mer, *J. Colloid Sci.* 23 (1958) 589.
- [44] T.W. Healy, V.K. La Mer, *J. Phys. Chem.* 66 (1962) 1835.
- [45] J.L. Ortega-Vinuesa, R. Hidalgo-Álvarez, F.J. de las Nieves, C.L. Davey, D.J. Newman, C.P. Price, *J. Colloid Interface Sci.* 204 (1998) 300.